ROS

RESEARCH ARTICLES

Radical Trapping Study of the Relaxation of *bis*-Fe(IV) MauG

Ian Davis[1,2], Teruaki Koto[1], and Aimin Liu[1,2]

[1]Department of Chemistry, University of Texas at San Antonio, San Antonio, TX 78249, USA; [2]Department of Chemistry, Georgia State University, Atlanta, GA 30303, USA

Correspondence: Feradical@utsa.edu (A.L.)

Davis I et al. Reactive Oxygen Species 5(13):46–55, 2018; ©2018 Cell Med Press
http://dx.doi.org/10.20455/ros.2018.801
(Received: September 5, 2017; Accepted: September 29, 2017)

ABSTRACT | The di-heme enzyme, MauG, utilizes a high-valent, charge-resonance stabilized *bis*-Fe(IV) state to perform protein radical-based catalytic chemistry. Though the *bis*-Fe(IV) species is able to oxidize remote tryptophan residues on its substrate protein, it does not rapidly oxidize its own residues in the absence of substrate. The slow return of *bis*-Fe(IV) MauG to its resting di-ferric state occurs *via* up to two intermediates, one of which has been previously proposed by Ma *et al.* (Biochem J 2016; 473:1769) to be a methionine-based radical in a recent study. In this work, we pursue intermediates involved in the return of high-valent MauG to its resting state in the absence of the substrate by EPR spectroscopy and radical trapping. The *bis*-Fe(IV) MauG is shown by EPR, HPLC, UV-Vis, and high-resolution mass spectrometry to oxidize the trapping agent, 5,5-dimethyl-1-pyrroline *N*-oxide (DMPO) to a radical species directly. Nitrosobenzene was also employed as a trapping agent and was shown to form an adduct with high-valent MauG species. The effects of DMPO and nitrosobenzene on the kinetics of the return to di-ferric MauG were both investigated. This work eliminates the possibility that a MauG-based methionine radical species accumulates during the self-reduction of *bis*-Fe(IV) MauG.

KEYWORDS | EPR spectroscopy; High-valent iron; Peroxide activation; Protein radical; Spin trapping

ABBREVIATIONS | DMPO, 5,5-dimethyl-1-pyrroline *N*-oxide; DMPOX, 5,5-dimethyl-2-oxo-pyrroline-1-oxyl; DMPOXH, 1-hydroxy-5,5-dimethylpyrrolidin-2-one; EPR spectroscopy, electron paramagnetic resonance spectroscopy; HPLC, high-performance liquid chromatography; NB, nitrosobenzene

CONTENTS

1. Introduction
2. Materials and Methods
   2.1. Chemicals
   2.2. Preparation of MauG
   2.3. UV-Visible Spectroscopy
   2.4. Electron Paramagnetic Resonance (EPR) Spectroscopy
   2.5. High-Performance Liquid Chromatography (HPLC) and High-Resolution Mass Spectrometry
3. Results

3.1. EPR Measurement of the Relaxation of *bis*-Fe(IV) MauG
3.2. Radical Trapping with DMPO
3.3. Identification of the Transient Radical
3.4. Radical Trapping with Nitrosobenzene
3.5. Effect of Spin Traps on the Kinetics of the Return to Resting State
4. Discussion

1. INTRODUCTION

MauG is a di-heme enzyme responsible for oxidizing two tryptophan residues on its substrate protein (preMADH) to produce the tryptophan tryptophylquinone cofactor of methylamine dehydrogenase [1]. In order to perform the oxidation reactions, MauG itself must first be oxidized to a high-valent *bis*-Fe(IV) state by hydrogen peroxide (H_2O_2) [2]. The heme moieties of MauG are inequivalent with distinct coordination environments: one five-coordinate and one six-coordinate [3]. Only the five-coordinate heme is able to react with H_2O_2, but the two heme centers are able to efficiently share electrons [2, 4, 5]. The substrate protein is oxidized by *bis*-Fe(IV) MauG through electron-hole hopping, generating tryptophan radicals on preMADH over a long distance [6, 7].

Even though *bis*-Fe(IV) MauG is electronically equivalent to the highly-reactive compound I of cytochrome P450 enzymes (an oxoferryl porphyrin cation radical), *bis*-Fe(IV) MauG is stable for several minutes at neutral pH [2, 8–10]. This unusual stability has been attributed to a type III charge-resonance phenomenon, by which the radical character of the high-valent species is shared over both hemes and with an intervening tryptophan residue [9, 10]. In the absence of its substrate, *bis*-Fe(IV) MauG will eventually return to its resting, di-ferric, state [11]. The return to the resting state is accompanied by oxidation of methionine residues on the surface of the protein adjacent to the buried five-coordinate heme center [12].

Recently, the mechanism by which *bis*-Fe(IV) MauG returns to the resting state has been studied kinetically [13]. It was shown through UV-Visible spectroscopy that MauG returns from its high-valent, *bis*-Fe(IV) state to its resting, di-ferric state *via* multiple intermediates: one at pH 7.4 and two at pH 9.0 [14]. As displayed in **Figure 1**, the first intermediate is proposed to be a protonated *bis*-Fe(IV) species, termed compound I-like. Intermediate I is only observed at basic pH values. The second intermediate, Intermediate II, is much longer lived and was proposed to be a single-electron reduced, mixed-valent species, termed compound II-like (i.e., an oxoferryl heme), with a one-electron oxidized methionine cation radical. A second electron transfer from methionine and proton from solvent to Intermediate II would then produce di-ferric MauG with an oxidized methionine residue. Protein-based radicals, particularly on tyrosine, tryptophan, and glycine residues, have been implicated in a large number of catalytic and electron transfer reactions in biology [15], including the long-range electron transfer reactions required for photosynthesis [16], respiration [17], and DNA synthesis [18] and repair [19]. Methionine oxidation by reactive oxygen species (ROS) and relevance to Alzheimer's disease has been proposed [20]. One electron chemical oxidation, irradiation, or photoreaction oxidation of free methionine amino acid or methionine residues in peptides has been studied computationally and experimentally [21–26]. Thus, it is highly significant to investigate the hypothesized methionine cation radical in MauG. In this work, we investigate the possibility of protein-based methionine radical involvement in the return of *bis*-Fe(IV) to di-ferric MauG.

2. MATERIALS AND METHODS

2.1. Chemicals

5,5-Dimethyl-1-pyrroline *N*-oxide (DMPO) was purchased from Cayman Chemical (Ann Arbor, MI, USA). All other chemicals, including nitrosobenzene, were purchased from Sigma Aldrich (St. Louis, MO, USA) at the highest available grade.

2.2. Preparation of MauG

MauG was prepared as described previously [1, 2, 4, 7, 9, 27]. Briefly, *P. denitrificans* cells carrying a

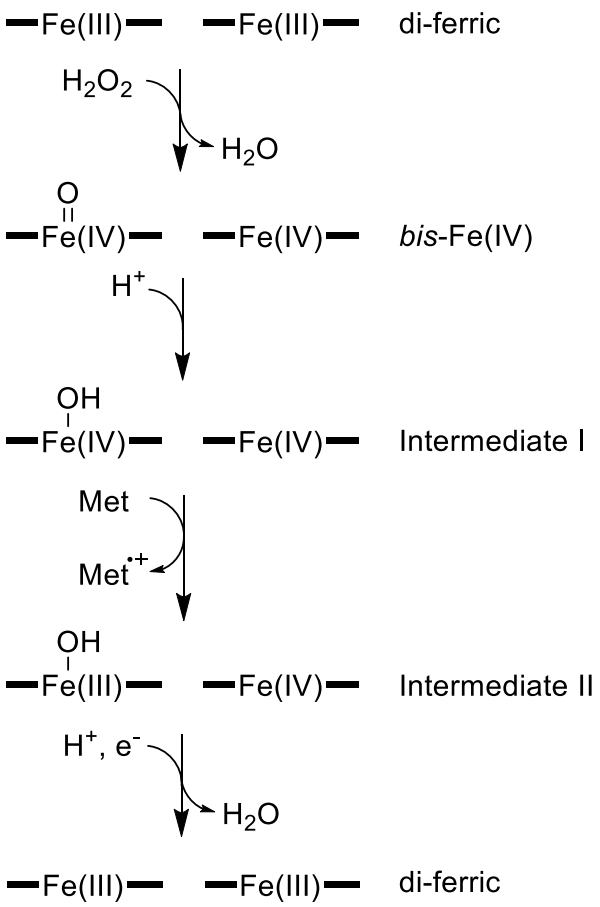

FIGURE 1. Various oxidation states of MauG. The scheme is based on the studies reported in Refs 13 and 14.

plasmid for expression of MauG were grown in mineral salts medium at 30ºC in 4 stages: 10 ml, 100 ml, 1 L, and 10 L. Tetracycline at 2 μg/ml was used for antibiotic selection. Cells were harvested by centrifugation, resuspended in phosphate buffer, and MauG was released from the periplasm by osmotic shock. Cell lysate was clarified by centrifugation, and the supernatant was collected. The His_6-tagged MauG was purified by nickel affinity chromatography, desalted to remove excess imidazole, and concentrated by ultrafiltration as described previously [7, 9, 27]. All reactions were carried out in 50 mM potassium phosphate buffered to pH 9.0 for optimized intermediate production.

2.3. UV-Visible Spectroscopy

The kinetics of the decay of *bis*-Fe(IV) MauG was measured with an Agilent 8453 spectrophotometer (Santa Clara, CA, USA). MauG and H_2O_2 were mixed to a final concentration of 5 μM each, and the return to the ground state was monitored in the absence and presence of DMPO (500 μM) from a fresh stock solution prepared under dark. As a precaution, the stock solution was subjected to multiple vacuum-argon cycles to remove potential trace amount of nitric oxide ($NO^{\bullet}$) from decayed spin trap but otherwise used without further purification.

2.4. Electron Paramagnetic Resonance (EPR) Spectroscopy

Room-temperature continuous-wave EPR spectra were collected in a quartz flat cell with a Bruker (Billerica, MA, USA) E560 spectrometer and Super-high-Q probehead (SHQE)-W resonator at 9.74 GHz, 100 kHz modulation frequency, 0.1 or 0.3 mT modulation amplitude, and 31.7 mW microwave power. Time courses were measured with 20 s per scan over a 10 mT sweep width at the $g = 2$ region.

2.5. High-Performance Liquid Chromatography (HPLC) and High-Resolution Mass Spectrometry

Chromatographic separation was performed with a Dionex UltiMate 3000 HPLC equipped with a diode array detector (Sunnyvale, CA, USA). The reaction mixture from the spin-trapping EPR experiment was applied to a C18 column and separation was achieved with a linear gradient of 100% solvent A (94.9% H_2O, 5% acetonitrile, and 0.1% trifluoroacetic acid) to 85% solvent A, 15% solvent B (94.9% acetonitrile, 5% H_2O, and 0.1% trifluoroacetic acid) over 7.5 min at 1.2 ml/min. Fractions were collected, and mass spectra were obtained on a maXis plus quadrupole-time of flight mass spectrometer equipped with an electrospray ionization source (Bruker Daltonics) operated in the positive ionization mode. Samples were introduced via syringe pump at a constant flow rate of 3 μl/min. Source parameters are summarized as follows: capillary voltage, 3500 V; nebulizer gas pressure, 0.4 bar; dry gas flow rate, 4.0 L/min; source temperature, 200°C. Mass spectra were averages of one minute of scans collected at a rate of 1 scan per second in the range $50 \leq m/z \leq$

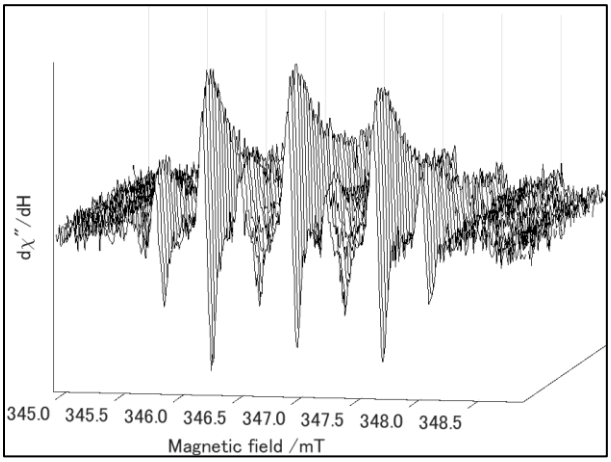

FIGURE 2. Time-resolved EPR spectra of *bis*-Fe(IV) MauG with DMPO. MauG (150 μM) was mixed with an equimolar concentration of H_2O_2 before adding DMPO (1.5 mM) and transferring the reaction mixture to a quartz flat cell. The first scan began 85 s after initial mixing, and a subsequent scan was recorded every ca. 23 s. The spectra were recorded at room temperature, 9.74 GHz, 31.7 mW microwave power, 100 kHz modulation frequency, 0.1 mT modulation amplitude, 10 mT sweep width, and 20 s sweep time.

1500. Compass Data Analysis software version 4.3 (Bruker Daltonics) was used to process all mass spectra.

3. RESULTS

3.1. EPR Measurement of the Relaxation of *bis*-Fe(IV) MauG

It was previously reported that at pH 9.0, the return to the resting state from *bis*-Fe(IV) requires more than 25 min and proceeds via two intermediates, the latter of which was proposed to be a methionine radical which maximizes at ~5 min after the formation of the high-valent species [14]. In order to investigate whether or not the auto-reduction of *bis*-Fe(IV) MauG involves a long-lived protein radical intermediate, the high-valent state of MauG (50 μM) was prepared by mixing with an equimolar amount of H_2O_2. The solution containing the *bis*-Fe(IV) MauG was then transferred to a quartz flat-cell, and the EPR spectrum at the g = 2 region was repeatedly scanned 30 times over 10 mins with 83 s having elapsed from the mixing of MauG with H_2O_2 and the beginning of the first scan. All scans are indistinguishable and contain only noise (data not shown). Since Intermediate I is expected to maximize at ca. 100 s and Intermediate II at 300 s, the absence of an EPR signal during the return of MauG from its high-valent to its resting state suggests that a stable protein radical is not involved.

3.2. Radical Trapping with DMPO

While the experiment described in section 3.1 above does not support the presence of a long-lived radical species during the conversion of *bis*-Fe(IV) MauG to the di-ferric state in the absence of substrate, it does not exclude the possibility of a transient, reactive radical being formed in the process. To test the possibility of a transient radical species being formed during the relaxation of *bis*-Fe(IV) MauG, the high-valent species of MauG (150 μM) was prepared by mixing with an equimolar amount of H_2O_2 and then mixed with DMPO (1.5 mM) before repeated EPR measurements with a dead time of 85 s between addition of the oxidant and the start of the first scan. Inclusion of DMPO during the relaxation process produces a 7-line EPR signal (**Figure 2**) which maximizes at ca. 160 s after mixing and then slowly decays. At the experimental pH of 9.0, MauG returns to the resting state via two intermediates. The appearance and decay of the transient EPR signal follows closely the first, Compound I-like, intermediate identified by UV-Vis spectroscopy [14]. To eliminate the second, Compound II-like, intermediate as the source of the EPR signal, a parallel experiment was performed in which the DMPO was added 300 s after the formation of *bis*-Fe(IV) MauG, at which point Intermediate I should be nearly gone and Intermediate II should be maximized. Samples made in this way show only a trace NO signal which is also seen in control samples of DMPO alone (**Figure 3A**, top).

3.3. Identification of the Transient Radical

The radical species observed can be simulated with a single component centered at g = 2.0068 with hyperfine interactions from one nitrogen nucleus, A_N = 20.0 MHz, and 2 equivalent protons, A_H = 11.0 MHz

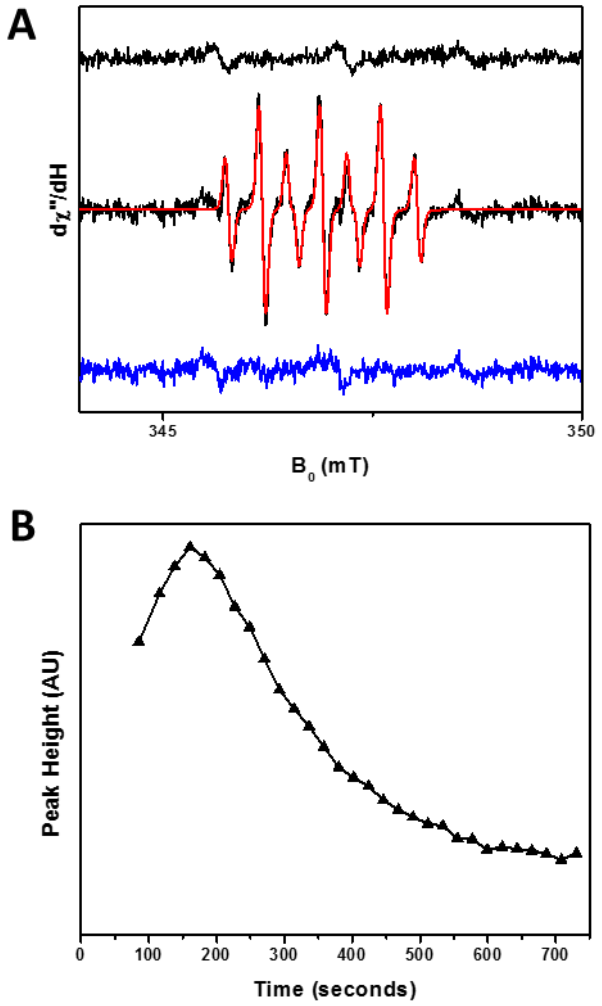

FIGURE 3. Identification of the transient radical species. (A) EPR spectrum of DMPO alone (top), the transient radical (middle, black), simulation (simulation parameters can be found in the text) (middle, red), and residual from fitting, bottom, blue; (B) Peak-to-trough height for the radical species over time. Spectrometer conditions are the same as in the legend of Figure 2.

(**Figure 3A**, middle) with a residual (**Figure 3A**, bottom) which is indistinguishable from the control, DMPO only (**Figure 3A,** top). The signals grow in and maximize at ~160 s, as seen in **Figure 3B**. These observations are inconsistent with a radical trapped by DMPO and are instead indicative of a radical of an oxidized DMPO product termed 5,5-dimethyl-2-oxo-pyrroline-1-oxyl (DMPOX) [28–31]. The presence of a DMPOX radical is further confirmed by performing chromatographic separation of the reaction mixture (**Figure 4A**) and analyzing the major fractions by high-resolution mass spectrometry. The second largest peak of the chromatogram has an absorbance maximum at 266 nm (**Figure 4B**) and shows one major ion by mass spectrometry which corresponds to a protonated DMPOX, 1-hydroxy-5,5-dimethylpyrrolidin-2-one (DMPOXH) within 3.07 ppm mass accuracy (**Figure 4C**).

3.4. Radical Trapping with Nitrosobenzene

Since the nitrone-based radical trap, DMPO, acts as a substrate for MauG, generating a DMPOX radical, we employed other spin traps in our attempts to trap the proposed methionine radical. **Figure 5** shows the EPR results with nitrosobenzene (NB) as an alternative spin trap. As can be seen in **Figure 5**, top two traces, respectively, di-ferric MauG and di-ferric MauG mixed with NB show no major resonances at room temperature. However, if NB is added after the formation of *bis*-Fe(IV), a new asymmetric radical species can be observed (**Figure 5**, 3rd trace). The spectrum can be simulated (blue) with a somewhat rhombic *g*-tensor, 2.00798, 2.00650, 2.00349, and a very anisotropic hyperfine coupling to one nitrogen atom, A_N 0.35, 22.2, 75.2 MHz, and 0.887 mT Gaussian line broadening. To determine whether the radical is localized on the protein or in solution, the sample was filtered with a 10 kDa cut-off centrifugal filter (MauG MW is 42 kDa) to separate the flow-through (**Figure 5**, 4th trace) and retained protein (**Figure 6**, 5th trace); the measurement was initiated 50 min after initial radical formation. Virtually no signal can be seen in the filtrate, and the retained protein shows approximately one-quarter of the initial intensity after re-dilution to the starting volume, though there is slightly less splitting in the low-field *g*-component. Thus, we conclude that the EPR signal is a protein-based radical. An additional experiment was performed in which NB was added 300 s after formation of *bis*-Fe(IV) MauG to assess the ability of Intermediate II to form an adduct (**Figure 5**, bottom trace). The delayed addition of NB leads to accumulation of less than 10% compared to direct addition, indicating that *bis*-Fe(IV) and Intermediate I are the most likely candidates for trapping with NB.

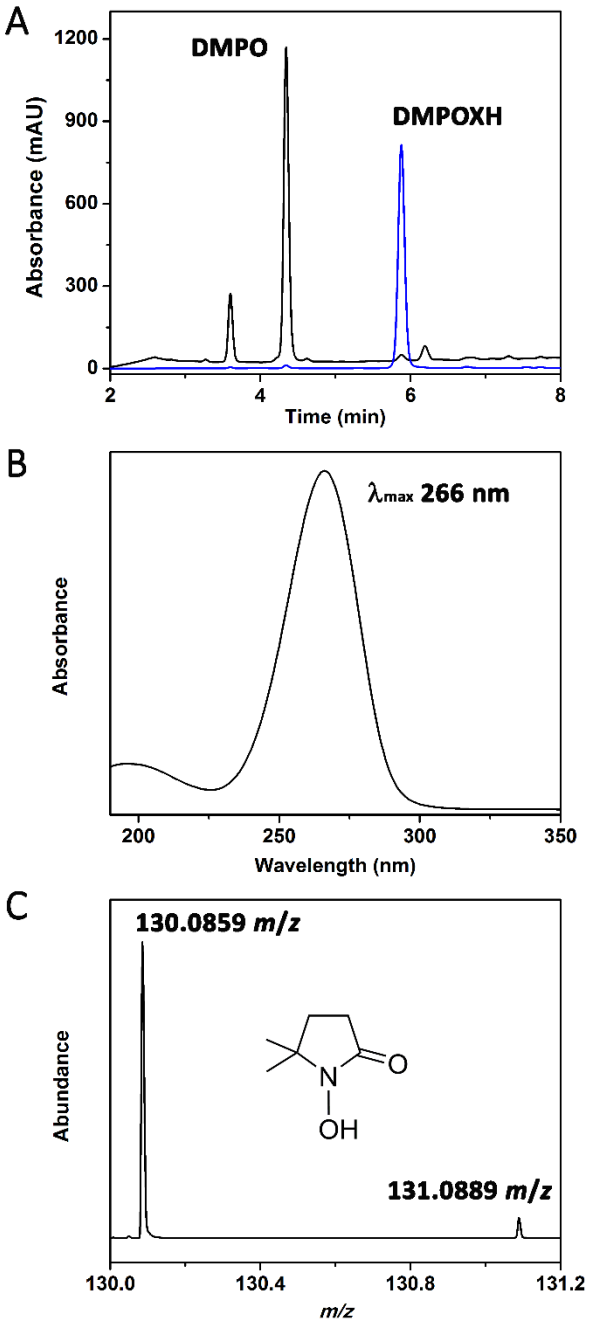

FIGURE 4. Characterization of the transient radical species. (A) HPLC chromatogram of the reaction mixture at 227 nm, black, and 266 nm, blue; (B) UV-Vis spectrum of the DMPOXH extracted from the chromatogram in A; (C) high-resolution mass spectrum of the peak corresponding to DMPOXH collected in positive ion mode.

3.5. Effect of Spin Traps on the Kinetics of the Return to Resting State

The decay of *bis*-Fe(IV) MauG was observed by UV-Visible spectroscopy alone and in the presence of nitrosobenzene and DMPO (**Figure 6** black, blue, and red, respectively). With MauG alone, the decay of the charge resonance band requires two summed exponential functions with rate constants of 0.83 ± 0.17 and 0.2 ± 0.04 min^{-1}, respectively. Addition of either spin trap immediately after the formation of *bis*-Fe(IV) resulted in a much faster return to the ground state. Additionally, while the data which includes spin traps show significant residuals from fitting with a single exponential, fits a double exponential equation do not converge and all parameters show complete dependency. The estimated rates with the inclusion of nitrosobenzene and DMPO are 0.94 ± 0.20 and 2.8 ± 0.5 min^{-1}, respectively. These results are consistent with high-valence forms of MauG being able to readily react with nitrosobenzene and DMPO.

4. DISCUSSION

Methionine residues are known to play a role in proteins as a sacrificial reductant to protect other, functionally important, residues from oxidative damage [32]. This appears to be the case in MauG, as it has three methionine residues on its surface which become oxidized as MauG redox cycles without the presence of its substrate [12]. The observation of two intermediates in the auto-reduction of *bis*-Fe(IV) MauG by UV-Vis spectroscopy makes MauG a promising candidate for the characterization or capture of a methionine radical in a protein. Previously characterized methionine radicals were generated photochemically with free amino acids, leaving an open question as to how a protein environment might affect a methionine radical [26, 33]. We sought to characterize or capture any possible radical species formed during the return of *bis*-Fe(IV) MauG to the resting state. Following the return to the di-ferric state by EPR spectroscopy did not produce any signals which could be attributed to a protein-based radical. We then attempted to trap any potential transient radical species with DMPO and NB. With DMPO, rather than trapping a protein-based radical, we observed that either *bis*-Fe(IV) MauG or Inter-

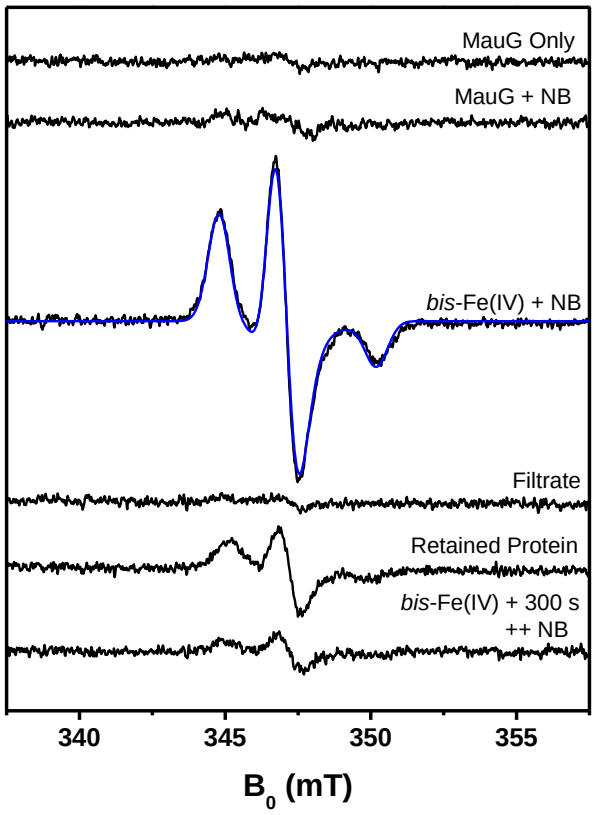

FIGURE 5. EPR of radical trapping with MauG and nitrosobenzene. From top to bottom, room temperature EPR spectra of MauG (50 μM), MauG mixed with NB (1 mM), a radical trapped by nitrosobenzene after mixing with *bis*-Fe(IV) MauG (black) and simulated spectrum (blue), parameters can be found in Section 3.4. The sample was then filtered by a 10 kDa spin filter. The next spectrum is the flow-through, followed by the filtered protein. The final spectrum contained bis-Fe(IV) aged for 300 s before addition of NB. Spectra were recorded at room temperature, 9.74 GHz, 31.7 mW microwave power, 100 kHz modulation frequency, 0.3 mT modulation amplitude, 30 mT sweep width, 80 s sweep time, and average of 4 scans.

mediate I is able to directly oxidize the spin trap to a DMPOX radical. We then attempted to trap a radical from Intermediate II by adding the trapping agent 300 s into the decay process, when Intermediate I should be nearly fully converted to Intermediate II. Delaying the addition of DMPO is able to remove the oxidation issue; however, no trapped radical species were observed. Furthermore, the rates of return from the *bis*-Fe(IV) to di-ferric state, as monitored by UV-Visible spectroscopy, were increased over 3-fold by the addition of DMPO.

The radical observed during the relaxation of *bis*-Fe(IV) MauG in the presence of DMPO does not agree with any published DMPO trapped radicals [31]. Rather, the radical arises from direct oxidation of DMPO to a so-called DMPOX species. The first published spectrum of the DMPOX radical arose in the attempt to trap a radical in the reaction of hematin with cumene hydroperoxide [29]. The assignment was made by comparison with a previously synthesized and characterized compound whose hyperfine coupling constants were reported in various solvents excluding any aqueous solutions [28]. Several similar compounds give rise to EPR signals with comparable coupling patterns and constants [34]. The rigorous assignment of the structure of the DMPOX radical was made later by direct synthesis and oxidation of DMPOX and measuring its EPR spectrum in various water/methanol mixtures [30]. It is also possible to produce the DMPOX radical from DMPO and singlet oxygen [35].

Even though DMPO is unable to trap any radicals within this system, NB is capable of rapidly forming an adduct with *bis*-Fe(IV) MauG or Intermediate I. The trapped radical is dissimilar to most radicals trapped with NB as it displays *g*-anisotropy at room temperature and only shows hyperfine coupling to a single nitrogen atom with extreme anisotropy, indicating that the *g*- and *A*-tensors may not coincide. A very similar species has been observed at liquid-nitrogen temperatures in an inorganic system [36], however their room temperature measurements are more similar to typical NB-trapped radicals with several coupled protons. Another study with a similarly-shaped radical signal at room temperature claimed to have used 2-methyl-2-nitrosopropane to trap a tyrosyl radical on cytochrome c [37]. The rapidness of the reaction between *bis*-Fe(IV) and NB indicates that the adduct is formed with *bis*-Fe(IV) or Intermediate I, both of which still carry two oxidizing equivalents. The absence of significant trapping at the later time suggests that NB is able to trap a radical on the tryptophan 199 of MauG which is responsible for passing oxidizing equivalents to its substrate protein.

In summary, though the reactive species of MauG returns to its resting state with two distinct intermediates, neither contains a long-lived protein radical. Furthermore, no radical adduct was able to be trapped by incubation of DMPO with *bis*-Fe(IV) MauG at various time points. Instead, the first intermediate is able to oxidize DMPO to produce a DMPOX radical while returning to its resting, di-ferric state. Conversely, NB is able to trap a radical with *bis*-Fe(IV) or Intermediate I MauG to form a long-lived radical with unusual spectral characteristics.

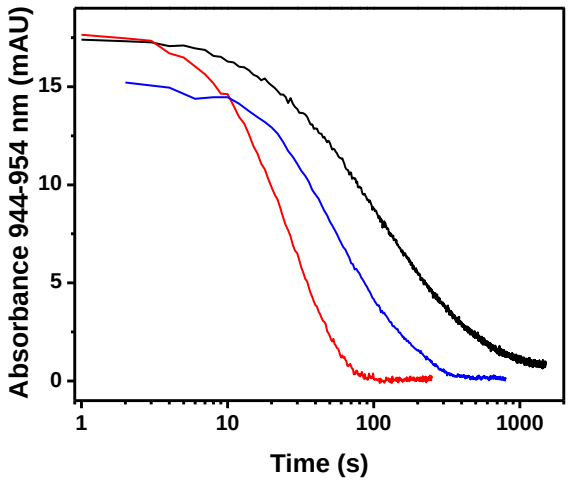

FIGURE 6. Kinetics of the decay of the charge resonance band of MauG. Representative time courses of the disappearance of the charge resonance band of *bis*-Fe(IV) as MauG returns to the resting, di-ferric state (black curve); the effect of nitrosobenzene (blue curve); and the effect of DMPO on the return to the resting state (red curve). Absorbance was averaged over 944–954 nm to improve the signal-to-noise ratio.

ACKNOWLEDGMENTS

This work was supported by the United Stated National Institutes of Health Grants GM108988 (to A.L.). The authors declare no conflicts of interest.

REFERENCES

1. Wang Y, Graichen ME, Liu A, Pearson AR, Wilmot CM, Davidson VL. MauG, a novel diheme protein required for tryptophan tryptophylquinone biogenesis. *Biochemistry* 2003; 42(24):7318–25. doi: 10.1021/bi034243q.
2. Li X, Fu R, Lee S, Krebs C, Davidson VL, Liu A. A catalytic di-heme *bis*-Fe(IV) intermediate, alternative to an Fe(IV)=O porphyrin radical. *Proc Natl Acad Sci USA* 2008; 105(25):8597–600. doi: 10.1073/pnas.0801643105.
3. Jensen LMR, Sanishvili R, Davidson VL, Wilmot CM. *In crystallo* posttranslational modification within a MauG/pre-methylamine dehydrogenase complex. *Science* 2010; 327(5971):1392–4.
4. Fu R, Liu F, Davidson VL, Liu A. Heme iron nitrosyl complex of MauG reveals an efficient redox equilibrium between hemes with only one heme exclusively binding exogenous ligands. *Biochemistry* 2009; 48(49):11603–5. doi: 10.1021/bi9017544.
5. Li XH, Feng ML, Wang YT, Tachikawa H, Davidson VL. Evidence for redox cooperativity between c-type hemes of MauG which is likely coupled to oxygen activation during tryptophan tryptophylquinone biosynthesis. *Biochemistry* 2006; 45(3):821–8.
6. Tarboush NA, Jensen LMR, Yukl ET, Geng J, Liu A, Wilmot CM, et al. Mutagenesis of tryptophan199 suggests that hopping is required for MauG-dependent tryptophan tryptophylquinone biosynthesis. *Proc Natl Acad Sci USA* 2011; 108(41):16956–61. doi: 10.1073/pnas.1109423108.
7. Yukl ET, Liu F, Krzystek J, Shin S, Jensen LMR, Davidson VL, et al. Diradical intermediate within the context of tryptophan tryptophylquinone biosynthesis. *Proc Natl Acad Sci USA* 2013; 110(12):4569–73. doi: 10.1073/pnas.1215011110.
8. Geng J, Davis I, Liu F, Liu A. Bis-Fe(IV): nature's sniper for long-range oxidation. *J Biol Inorg Chem* 2014; 19(7):1057–67. doi: 10.1007/s00775-014-1123-8.
9. Geng J, Dornevil K, Davidson VL, Liu A. Tryptophan-mediated charge-resonance stabilization in the *bis*-Fe(IV) redox state of MauG. *Proc Natl Acad Sci USA* 2013;

110(24):9639–44. doi: 10.1073/pnas.1301544110.
10. Geng J, Davis I, Liu A. Probing *bis*-Fe(IV) MauG: Experimental evidence for the long-range charge-resonance model. *Angew Chem Intl Ed* 2015; 54(12):3692–6. doi: 10.1002/anie.201410247.
11. Shin S, Lee S, Davidson VL. Suicide inactivation of MauG during reaction with O_2 or H_2O_2 in the absence of its natural protein substrate. *Biochemistry* 2009; 48(42):10106–12. doi: 10.1021/bi901284e.
12. Yukl ET, Williamson HR, Higgins L, Davidson VL, Wilmot CM. Oxidative damage in MauG: implications for the control of high-valent iron species and radical propagation pathways. *Biochemistry* 2013; 52(52):9447–55. doi: 10.1021/bi401441h.
13. Ma Z, Williamson HR, Davidson VL. Roles of multiple-proton transfer pathways and proton-coupled electron transfer in the reactivity of the *bis*-Fe(IV) state of MauG. *Proc Natl Acad Sci USA* 2015; 112(35):10896–901. doi: 10.1073/pnas.1510986112.
14. Ma Z, Williamson Heather R, Davidson Victor L. Mechanism of protein oxidative damage that is coupled to long-range electron transfer to high-valent haems. *Biochem J* 2016; 473(12):1769.
15. Stubbe J, van der Donk WA. Protein radicals in enzyme catalysis. *Chem Rev* 1998; 98(2):705–62.
16. Nelson N, Yocum CF. Structure and function of photosystems I and II. *Annu Rev Plant Biol* 2006; 57:521–65. doi: 10.1146/annurev.arplant.57.032905.105350.
17. Svistunenko DA, Wilson MT, Cooper CE. Tryptophan or tyrosine? On the nature of the amino acid radical formed following hydrogen peroxide treatment of cytochrome *c* oxidase. *Biochim Biophys Acta* 2004; 1655(1–3):372–80. doi: 10.1016/j.bbabio.2003.06.006.
18. Stubbe J, Nocera DG, Yee CS, Chang MC. Radical initiation in the class I ribonucleotide reductase: long-range proton-coupled electron transfer? *Chem Rev* 2003; 103(6):2167–201. doi: 10.1021/cr020421u.
19. Aubert C, Vos MH, Mathis P, Eker APM, Brettel K. Intraprotein radical transfer during photoactivation of DNA photolyase. *Nature* 2000; 405(6786):586–90.
20. Schoeneich C. Methionine oxidation by reactive oxygen species: reaction mechanisms and relevance to Alzheimer's disease. *Biochim Biophys Acta* 2005; 1703(2):111–9. doi: 10.1016/j.bbapap.2004.09.009.
21. Pogocki D, Burlinska G, Wasowicz T, Sadlo J, Bobrowski K. Radical induced oxidation of sulfur-containing amino acids. an ESR study. *Mol Phys Rep* 1994; 6:224–9.
22. Goez M, Rozwadowski J. Reversible pair substitution in CIDNP: the radical cation of methionine. *J Phys Chem A* 1998; 102(41):7945–53. doi: 10.1021/JP981791I.
23. Pogocki D, Serdiuk K, Schoeneich C. Computational characterization of sulfur-oxygen three-electron-bonded radicals in methionine and methionine-containing peptides: important intermediates in one-electron oxidation processes. *J Phys Chem A* 2003; 107(36):7032–42. doi: 10.1021/jp034811b.
24. Zhao J, Ng CMD, Chu IK, Siu KWM, Hopkinson AC. Methionine, α-methylmethionine and *S*-methylcysteine radical cations: generations and dissociations in the gas phase. *Phys Chem Chem Phys* 2009; 11(35):7629–39. doi: 10.1039/b905615g.
25. Fourre I, Berges J, Houee-Levin C. Structural and topological studies of methionine radical cations in dipeptides: electron sharing in two-center three-electron bonds. *J Phys Chem A* 2010; 114(27):7359–68. doi: 10.1021/jp911983a.
26. Yashiro H, White RC, Yurkovskaya AV, Forbes MDE. Methionine radical cation: structural studies as a function of pH using X- and Q-band time-resolved electron paramagnetic resonance spectroscopy. *J Phys Chem A* 2005; 109(26):5855–64. doi: 10.1021/jp051551k.
27. Geng J, Huo L, Liu A. Heterolytic O-O bond cleavage: functional role of Glu113 during *bis*-Fe(IV) formation in MauG. *J Inorg Biochem* 2017; 167:60–7. doi: 10.1016/j.jinorgbio.2016.11.013.
28. Aurich HG, Trosken J. Losungsmittelabhangigkeit der ESR-spektren von alkyl-acyl-nitroxiden. *Liebigs Ann Chen* 1971; 745:159–63.
29. Floyd RA, Soong LM. Spin trapping in biological systems: oxidation of the spin trap 5,5-dimethyl-1-pyrroline-1-oxide by a hydroperoxide-hematin system. *Biochem Biophys Res Commun* 1977; 74(1):79–84. doi:

10.1016/0006-291X(77)91377-8.
30. Rosen GM, Rauckman EJ. Spin trapping of the primary radical involved in the activation of the carcinogen *N*-hydroxy-2-acetylaminofluorene by cumene hydroperoxide-hematin. *Mol Pharmacol* 1980; 17(2):233–8.
31. Buettner GR. Spin trapping: ESR parameters of spin adducts. *Free Radic Biol Med* 1987; 3(4):259–303. doi: 10.1016/S0891-5849(87)80033-3.
32. Stadtman ER, Levine RL. Free radical-mediated oxidation of free amino acids and amino acid residues in proteins. *Amino Acids* 2003; 25(3):207–18. doi: 10.1007/s00726-003-0011-2.
33. Makino K. Studies on spin-trapped radicals in .gamma-irradiated aqueous solutions of DL-methionine by high performance liquid chromatography and ESR spectroscopy. *J Phys Chem* 1979; 83(19):2520–3. doi: 10.1021/j100482a020.
34. Mackor A, Wajer TAJW, de Boer TJ. C-Nitroso compounds—VI. *Tetrahedron* 1968; 24(4):1623–31. doi: 10.1016/S0040-4020(01)82469-8.
35. Bilski P, Reszka K, Bilska M, Chignell CF. Oxidation of the spin trap 5,5-dimethyl-1-pyrroline *N*-oxide by singlet oxygen in aqueous solution. *J Am Chem Soc* 1996; 118(6):1330–8. doi: 10.1021/ja952140s.
36. Neidlinger A, Kienz T, Heinze K. Spin trapping of carbon-centered ferrocenyl radicals with nitrosobenzene. *Organometallics* 2015; 34(21):5310–20. doi: 10.1021/acs.organomet.5b00778.
37. Qian SY, Chen YR, Deterding LJ, Fann YC, Chignell CF, Tomer KB, et al. Identification of protein-derived tyrosyl radical in the reaction of cytochrome c and hydrogen peroxide: characterization by ESR spin-trapping, HPLC and MS. *Biochem J* 2002; 363(Pt 2):281–8.